Supporting Information:

Infrared Spectra and Hydrogen-Bond Configurations of Water Molecules at the Interface of Water-Insoluble Polymers under Humidified Conditions

Yuka Ikemoto,[*1] Yoshihisa Harada,[2,3] Masaru Tanaka,[4,5] Shin-nosuke Nishimura,[4,†] Daiki Murakami,[4,5,††] Naoya Kurahashi,[2,3] Taro Moriwaki,[1] Kosuke Yamazoe,[2,3,†††] Hitoshi Washizu,[6] Yoshiki Ishii,[6] and Hajime Torii[*7]

[1] *Japan Synchrotron Radiation Research Institute, Spectroscopy Division, 1-1-1 Kouto Sayo, Hyogo 679-5198, Japan*

[2] *Institute for Solid State Physics, The University of Tokyo, Kashiwa, Chiba 277-8581, Japan*

[3] *Synchrotron Radiation Research Organization, The University of Tokyo, Bunkyo-ku, Tokyo 113-8656, Japan*

[4] *Institute for Materials Chemistry and Engineering, Kyushu University, 744 Motooka, Nishi-ku, Fukuoka 819-0395, Japan*

[5] *Graduate School of Engineering, Kyushu University, 744 Motooka, Nishi-ku, Fukuoka 819-0395, Japan*

[6] *Graduate School of Information Science, University of Hyogo, 7-1-28 Minatojima-Minamimachi, Chuo-ku, Kobe, Hyogo 650-0047, Japan*

[7] *Department of Applied Chemistry and Biochemical Engineering, Faculty of Engineering, and Department of Optoelectronics and Nanostructure Science, Graduate School of Science and Technology, Shizuoka University, 3-5-1 Johoku, Naka-ku, Hamamatsu 432-8561, Japan*

† Present address: Faculty of Science and Engineering, Department of Molecular Chemistry and Biochemistry, Doshisha University, 1-3 Tatara Miyakodani, Kyotanabe, Kyoto 610-0394, Japan

†† Present address: Department of Biological and Environmental Chemistry, Faculty of Humanity-Oriented Science and Engineering, Kindai University, 11-6 Kayanomori, Iizuka, Fukuoka, 820-8555, Japan

††† Present address: Japan Synchrotron Radiation Research Institute, 1-1-1 Kouto, Sayo, Hyogo 679-5198, Japan

***** Corresponding authors. Email: ikemoto@spring8.or.jp; torii.hajime@shizuoka.ac.jp

Contents

1. **Properties of Polymers**
2. **Synthesis of poly(2-methoxyethyl acrylate) (PMEA) and poly(*n*-butyl acrylate) (PBA)**
3. **Method of Infrared Spectroscopy**
4. **Estimation of the Adsorbed Water under Humidified Condition**
5. **IR Spectra at Dry Condition**
6. **Structural Characteristics of the Complexes Considered in the Theoretical Calculations**
7. **Behavior of the Frequency Shifts Calculated for the Acetone...Water and Dimethyl Ether...Water 1:1 Complexes (Types 2a and 2e)**

1. Properties of Polymers

Polymers examined in the present study are poly(2-methoxyethyl acrylate) (PMEA),[S1, S2] cyclic(poly(2-methoxyethyl acrylate) (cyclic-PMEA),[S3] and poly(*n*-butyl acrylate) (PBA).[S1, S2] The number-average molecular weight (M_n) and polydispersity index ($Đ \equiv M_w/M_n$, where M_w is weight-average molecular weight) were M_n = 38000 g mol^{-1} and $Đ$ = 1.17 for PMEA, M_n = 76000 g mol^{-1} and $Đ$ = 1.06 for cyclic-PMEA, M_n = 42000 g mol^{-1} and $Đ$ = 1.19 for PBA. Saturated water contents are 8.7 wt%, 12.2 wt%, and 1.9 wt% for PMEA, cyclic-PMEA, and PBA. These values correspond to the average number of 0.78, 1.1, and 0.16, respectively, of water molecules per monomer. The protein or platelet adsorption is high for PBA, and low for PMEA and cyclic-PMEA. The DSC thermograms of PMEA and cyclic-PMEA have cold crystallization peaks, the origin of which is defined as intermediate water, but that of PBA has no such peak. The water contact angle, which is one of the indicators of hydrophilic or hydrophobic properties, is 39.3°, 83.5°, and 81.1°for PMEA, cyclic-PMEA, and PBA.

A polymer was casted on a silicon wafer for IR measurements. A toluene solution of the polymers (0.8 mg mL^{-1}, 300 mL) was cast-coated at ambient temperature for 6 h. The obtained polymer films were dried in *vacuo* at 30 °C for overnight. Dust particles in the polymer solution were removed by filtration using a DISMIC-13JP (Toyo Roshi Kaisha, Ltd., material: PTFE, pore size: 0.20 mm).

2. Synthesis of poly(2-methoxyethyl acrylate) (PMEA) and poly(*n*-butyl acrylate) (PBA)

The PMEA and PBA with narrow dispersity used in this study were synthesized by reversible addition-fragmentation chain transfer (RAFT) polymerization according to our previous report.[S4] RAFT-synthesized polymers contain a chain transfer group, such as trithiocarbonate[S4] and dithioester,[S5,S6] on the chain end. The chain end groups often affect the hydration behavior and physical property of polymers. To defuse this effect, we carried out radical-induced reduction desulfurization for the RAFT-synthesized PMEA and PBA. The polymers 0.5 g, 20 equivalent of tris(trimethylsilyl)silane (Tokyo Chemical Industries Co., Ltd.,

Japan), and 0.5 equivalent of 2,2'-azobis(4-methoxy-2,4-dimethylvaleronitrile) (FUJIFILM Wako Pure Chemical Co., Ltd., Japan) were dissolved into 2 mL toluene (Kanto Chemicals Co. Inc., Japan). The yellow-colored-solutions were deoxygenated by freeze-pump-thaw cycles under dry Ar gas. Then the reaction mixtures were stirred for 12 h at 40 °C, resulting in colorless solutions. After undergoing reduction, the mixtures were poured into a large excess of hexane (Kanto Chemicals Co. Inc., Japan) for PMEA and methanol (Kanto Chemicals Co. Inc., Japan) for PBA to precipitate the resulting polymers. The polymers were further purified via reprecipitation using the tetrahydrofuran (Kanto Chemicals Co. Inc., Japan)/hexane (for PMEA) and tetrahydrofuran/methanol (for PBA) systems. The solvents were removed in vacuo to obtain pure desulfurized-PMEA and PBA as a colorless viscous liquid. The progresses of chain end removal were confirmed by nuclear magnetic resonance spectroscopies.[S4]

3. Method of Infrared Spectroscopy

IR spectra (in the mid-IR region from 600 to 8000 cm^{-1}) were measured on the IR beamline BL43IR at SPring-8 synchrotron facility (Hyogo, Japan). An FTIR microspectrometer (BRUKER model HYPERION IR microscope with model VERTEX70 FTIR spectrometer) was used with the IR synchrotron radiation. The wavenumber resolution was 2 cm^{-1} and accumulated number was 100. The humidity dependence of absorption spectra was measured using a humidity controlling cell. The schematic illustration of the cell is shown in Figure S1. The atmosphere in the cell was controlled by a mixing device (RIGAKU model HUM-1E), which mixes N_2 gas (99.99%, generated by a KOFLOC model MNT- 0.8SI nitrogen gas generator) and water vapor at the specified ratio.[S7] The water used in the mixing device was purified through a Millipore model Elix advantage-3 water purifier. There is a KRS-5 window at the top of the cell. The relative humidity (RH) and the temperature in the cell were monitored by a sensor (Sensirion model SHT35). The temperature was 26 °C. A polymer casted silicon wafer was on the bottom of the cell. The thickness of the film was about 2 μm. The wafer was double-sided polishing N-type one, and the thickness, resistivity, and face orientation were 500 μm, >1000 Ω cm, and (100). The sample spectra were measured about 5 minutes after the value of the humidity was set up to each value. The background spectrum was measured without setting the sample in the humidified cell and was used to cancel the features of the water in the upper spatial region from the absorption spectrum of the sample. In order to calibrate the polymer thickness, the observed absorption spectra were normalized by the integrated intensity of the C=O stretching band.

4. Estimation of the Amount of Adsorbed Water under Humidified Condition

The amount of water adsorbed into the polymers was estimated using the IR spectra. For this purpose, we prepared water saturated PMEA and PBA. The amount of water per monomer unit of these polymers was calculated by the weight to be 0.74 and 0.16 for PMEA and PBA, respectively. The ATR-IR spectra of them were measured by FT-IR spectrometer (JASCO model FT/IR-6600, 45° incidence Ge-ATR), and

penetration depth correction was applied. From these ATR-IR spectra, the ratio of the integrated intensity of the OH stretching band to that of the C=O stretching band was calculated. Then, by comparing them with the IR absorption spectra measured under humidified condition, the amount of water molecules adsorbed into these two polymers at each RH% was calculated. The amount of water adsorbed into cyclic-PMEA was estimated with reference to that obtained for PMEA. The average number of adsorbed water molecules per monomer under humidified condition is listed in Table S1.

5. IR Spectra at Dry Condition

Figure S2 shows the absorption spectra of PMEA, cyclic-PMEA and PBA at dry condition. The wavenumbers of the major peaks of the PMEA spectrum are labeled in the figure. The spectral shape of cyclic-PMEA is essentially the same as that of PMEA. Note that cyclic-PMEA has a ring shape with the polymer main chain termini connected to each other. Since the ring is very large and the difference in the molecular structure is only in the way of main chain termination, it is reasonable that the shape of the spectrum is essentially the same. In contrast, in the spectrum of PBA, the structures below 1130 cm^{-1} are significantly weaker than those in the spectra of PMEA and cyclic-PMEA. The band assignments of all these spectra may be made rather empirically as follows.[S8, S9] The bands observed from 2800 to 3000 cm^{-1} are assigned to the CH stretching modes. More specifically, the CH_3 asymmetric and CH_2 antisymmetric stretching vibrations are observed at 2986 and 2940 cm^{-1}, respectively, while the symmetric stretching modes of these groups are observed at 2888 and 2819 cm^{-1}. The band at 1736 cm^{-1} is assigned to the C=O stretching mode. The CH deformation vibrations are observed at 1450, 1253, and 854 cm^{-1}. The band at 1168 cm^{-1} is assigned to the stretching mode of C–O–C in the ester group. The bands at 1130 and 1032 cm^{-1} originate from the stretching modes of C–O–C in the ether group. PBA has no ether group, and there is no band at these wavenumbers in its spectrum. We point out that the absorption spectra of dry samples in Figure S2 have no obvious band at about 3400 and 1635 cm^{-1} at which the OH stretching and bending vibrations of water are observed.

6. Structural Characteristics of the Complexes Considered in the Theoretical Calculations

For types 1a and 1e, calculations were carried out for six and four complexes, respectively, shown in Figure S3 to cover a variety of possible hydrogen-bond configurations, including a bifurcated configuration and a (topologically) linear hydrogen-bond chain of water. For type 2a, the structure of each complex was optimized with θ (defined as 180° minus the C=O...H angle) and φ [the C(methyl)–C=O...H dihedral angle] being fixed at specified values: θ = 0°, (θ, φ) = (90°, 0–90°), (2–89°, 0°), (2–89°, 90°) [taken with the interval of $\Delta\varphi$ or $\Delta\theta$ = 1°], as well as about 2000 sets of (θ, φ) taken randomly within the range of 1.5° ≤ θ ≤90° and 0° ≤ φ ≤ 90°. The angles were defined in this way so that they are the inclination and azimuth of the spherical polar coordinate system with the origin being taken at the carbonyl O atom and z being taken along the C=O bond. The situation is similar for type 2e, but the z axis was taken along the C–O–C bisection, and some of the sets of (θ, φ) were excluded due to the steric hindrance between water and one

of the methyl groups. For these two types, it is supposed[S10,S11] that constraints on softer modes (C=O...H bending and C–C=O...H torsion for type 2a, and similar modes relative to the C–O–C bisection for type 2e) do not essentially have any harmful effect on the properties of harder modes (OH stretches). For types 3a and 3e, a few (up to four) water molecules at the center of the $(water)_{90}$ clusters (13 structures in total)[S12,S13] were replaced by an acetone or dimethyl ether molecule, and then the structure was fully optimized. For type 4, the complexes shown in Figure S4 were considered to examine the vibrational properties that are characteristic of bridging hydrogen-bond configurations.

7. Behavior of the Frequency Shifts Calculated for the Acetone...Water and Dimethyl Ether...Water 1:1 Complexes (Types 2a and 2e)

As shown in Figure S6 (b), the frequency (of HDO) is calculated as 3622 cm^{-1} at $\theta = 0°$ (linear C=O...H configuration), and shifts to the low-frequency side as θ increases to ~60°. In fact, the extent of the frequency shift is the largest at $\varphi = 0°$, where the H atom of water is located on the plane of the carbonyl group, and is the smallest at $\varphi = 90°$, where the H atom of water is located out of the plane. (The dependence on φ is explicitly shown as 3D plots in Figure S7.) This is related to the dependence of the hydrogen-bond distance on the θ and φ angles shown in Figure S6 (a). A similar dependence is also recognized for the lower-frequency OH stretch (corresponding to the OH symmetric stretch of an isolated water molecule) of the normal isotopic species as shown in Figure S6 (c). Around $\theta = 90°$, the frequency increases and the hydrogen-bond distance is elongated partly because of intrinsically weaker hydrogen-bond interaction and partly because of steric hindrance between water and one of the methyl groups.

In the case of the complexes of type 2e (dimethyl ether...water 1:1 complexes), the steric hindrance between water and one of the methyl groups is more severe because the hydrogen-bond acceptor is not sticking out of the rest of the molecule, resulting in the dependence of the frequencies and the hydrogen-bond distance on the θ and φ angles as shown in Figures S6 (d–f) and S8. (The complexes with hydrogen-bond distances longer than 2.6 Å were excluded in the calculations.) However, when the frequencies are plotted against the hydrogen-bond distance as shown in Figure S6 (g) and (h), it is seen that the distributions of the frequencies at each hydrogen-bond distance are narrower for type 2e than those for type 2a.

References

(S1) Tanaka, M.; Mochizuki, A. Effect of Water Structure on Blood Compatibility – Thermal Analysis of Water in Poly(meth)acrylate. *J. Biomed . Mater. Res. A.* **2004**, *68A*, 684-695.

(S2) Kobayashi, S.; Wakui, M.; Iwata, Y.; Tanaka, M. Poly(ω-methoxyalkyl acrylate)s: Nonthrombogenic Polymer Family with Tunable Protein Adsorption. *Biomacromolecules* **2017**, *18*, 4214-4223.

(S3) Nishimura, S.; Ueda, T.; Murakami, D.; Tanaka, M. Chain-End Effect for Intermediate Water Formation of Poly(2-Methoxyethyl Acrylate). *Organic Materials* **2021**, *3*, 214-220.

(S4) Murakami, D.; Yamazoe, K.; Nishimura, S.; Kurahashi, N.; Ikemoto, Y.; Miyawaki, J.; Tanaka, M.; Harada, Y. Hydration Mechanism in Blood-Compatible Polymers Undergoing Phase Separation. *Langmuir* **2022**, *38*, 1090–1098.

(S5) Nishimura, S.; Hokazono, N.; Taki, Y.; Motoda, T.; Morita, Y.; Yamamoto, K.; Higashi, N.; Koga. T. Photocleavable Peptide–Poly(2-hydroxyethyl methacrylate) Hybrid Graft Copolymer via Postpolymerization Modification by Click Chemistry to Modulate the Cell Affinities of 2D and 3D Materials. *ACS Appl. Mater. Interfaces* **2019**, *11*, 24577–24587.

(S6) Higashi, N.; Narimatsu, K.; Okumura, M.; Nishimura, S.; Koga, T. Spontaneous Formation of Nanoparticles from Peptide–Vinyl Polymer Diblock Hybrids Prepared by RAFT Polymerization and Their Interactions with Cells. *ACS Omega* **2019**, *4*, 8104–8111.

(S7) Baba, S.; Hoshino, T.; Ito, L.; Kumasaka, T. Humidity Control and Hydrophilic Glue Coating Applied to Mounted Protein Crystals Improves X-ray Diffraction Experiments. *Acta Crystallogr. D. Biol. Crystallogr.* **2013**, *D69*, 1839–1849.

(S8) Guan, L.; Xu, H.; Huang, D. The Investigation on States of Water in Different Hydrophilic Polymers by DSC and FTIR. *J. Polym. Res.* **2011**, *18*, 681-689.

(S9) Socrates, G. *Infrared and Raman Characteristic Group Frequncies: Tables and Charsts,* 3rd ed.; John Wiley & Sons, 2004.

(S10) Torii, H. Amide I Vibrational Properties Affected by Hydrogen Bonding Out-of-Plane of the Peptide Group. *J. Phys. Chem. Lett.* **2015**, *6*, 727−733.

(S11) Torii, H.; Kawanaka, M. Secondary Structure Dependence and Hydration Effect of the Infrared Intensity of the Amide II Mode of Peptide Chains. *J. Phys. Chem. B* **2016**, *120*, 1624−1634.

(S12) Torii, H.; Ukawa, R. Role of Intermolecular Charge Fluxes in the Hydrogen-Bond-Induced Frequency Shifts of the OH Stretching Mode of Water. *J. Phys. Chem. B* **2021**, *125*, 1468–1475.

(S13) Torii, H. Singular Value Decomposition Analysis of the Electron Density Changes Occurring upon Electrostatic Polarization of Water. *RSC Adv.* **2022**, *12*, 2564–2573.

Supplementary table

Table S1. Estimated average number of adsorbed water molecules per monomer at each RH.

	average number of adsorbed water molecules per monomer			
polymer	at 50–53%RH	at 72–75%RH	at 85–90%RH	at 98%RH
PMEA	0.05, 52%RH	0.08, 72%RH	0.17, 90%RH	0.27, 98%RH
cyclic-PMEA	0.05, 53%RH	0.09, 75%RH	0.16, 85%RH	0.44, 98%RH
PBA	<0.01, 50%RH	--	--	0.01, 98%RH

Supplementary figures

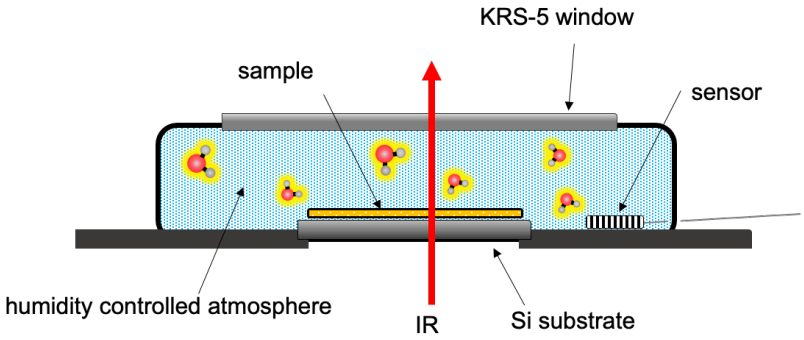

Figure S1. Schematic illustration of the humidity controlling cell.

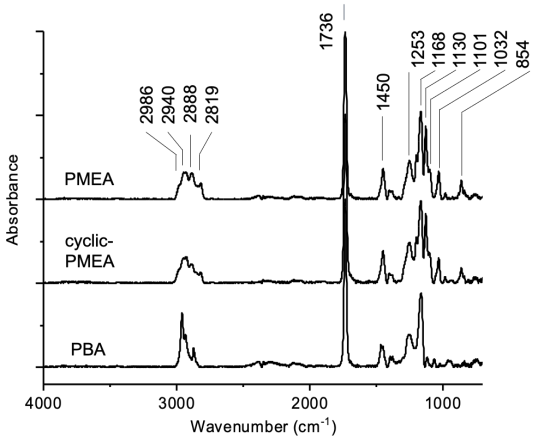

Figure S2. Absorption spectra of PMEA, cyclic-PMEA and PBA at dry condition.

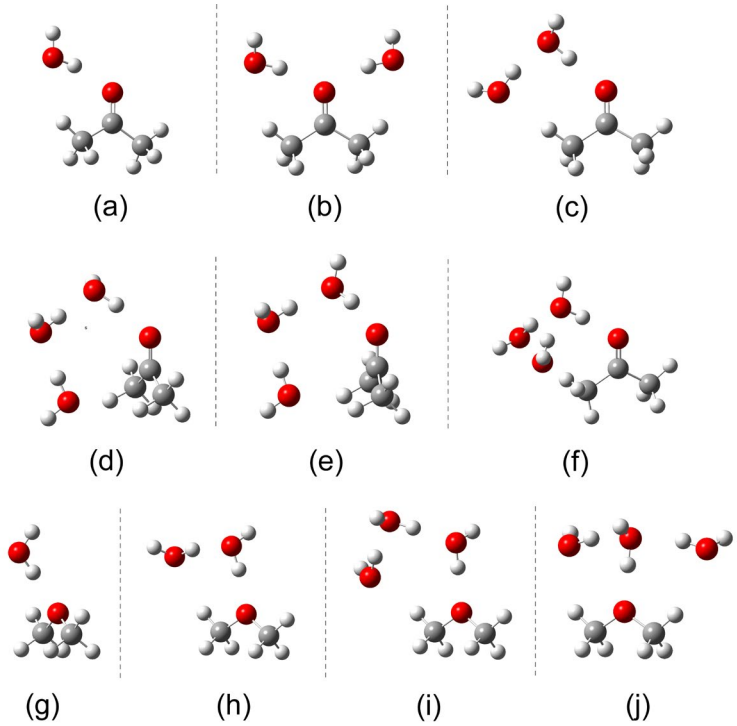

Figure S3. Structures of the complexes of (a–f) type 1a and (g–j) type 1e considered in the present study.

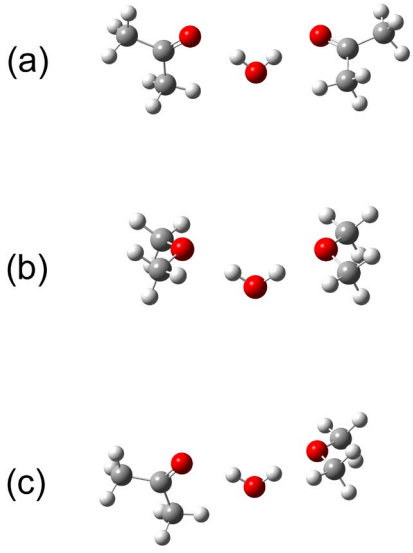

Figure S4. Structures of the complexes of type 4 considered in the present study.

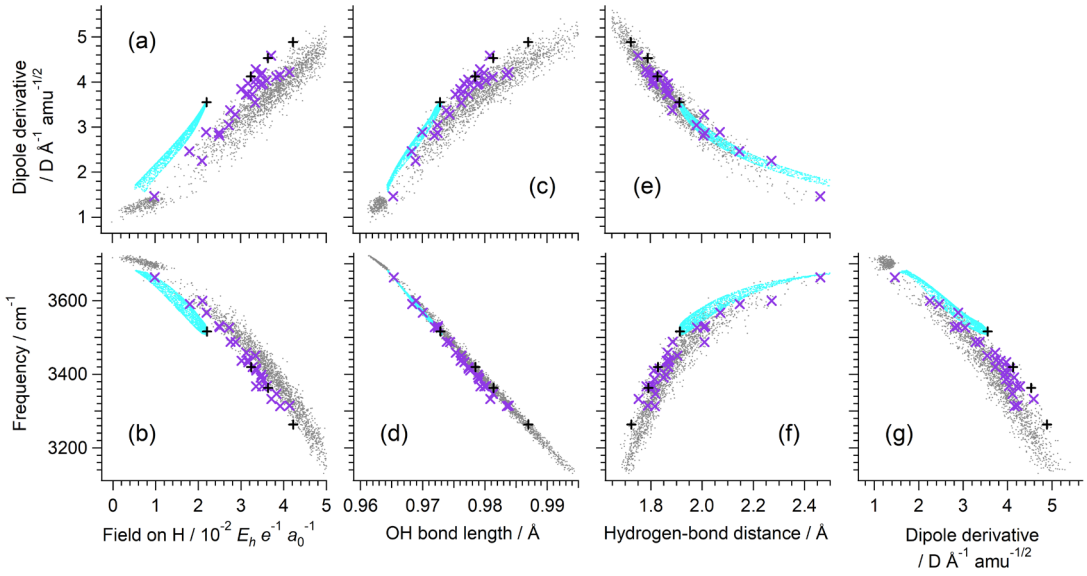

Figure S5. Plots of the (a,c,e) dipole derivative and (b.d.f.g) vibrational frequency (scaled) of the OH stretching mode against the (a,b) electric field on the vibrating hydrogen atom (the component along the OH bond), (c,d) OH bond length, (e,f) hydrogen-bond distance, and (g) dipole derivative of the OH stretching mode calculated for the dimethyl ether + $n$$H_2O$ complexes (n = 1–3, with full geometry optimization, black +), the dimethyl ether + H_2O complexes with variously fixed angular hydrogen-bond configurations (light blue dots), and the complexes of dimethyl ether buried in a cavity made around the center of the $(water)_{90}$ clusters with full geometry optimization (purple ×), overlapped on the results obtained[S12] for the OH stretches of the $(water)_{90}$ clusters (gray dots). With regard to the complexes involving dimethyl ether the stretching of the OH bond directly interacting with dimethyl ether is considered, and [including the case of the $(water)_{90}$ clusters] the hydrogen atoms other than the vibrating one are deuterated.

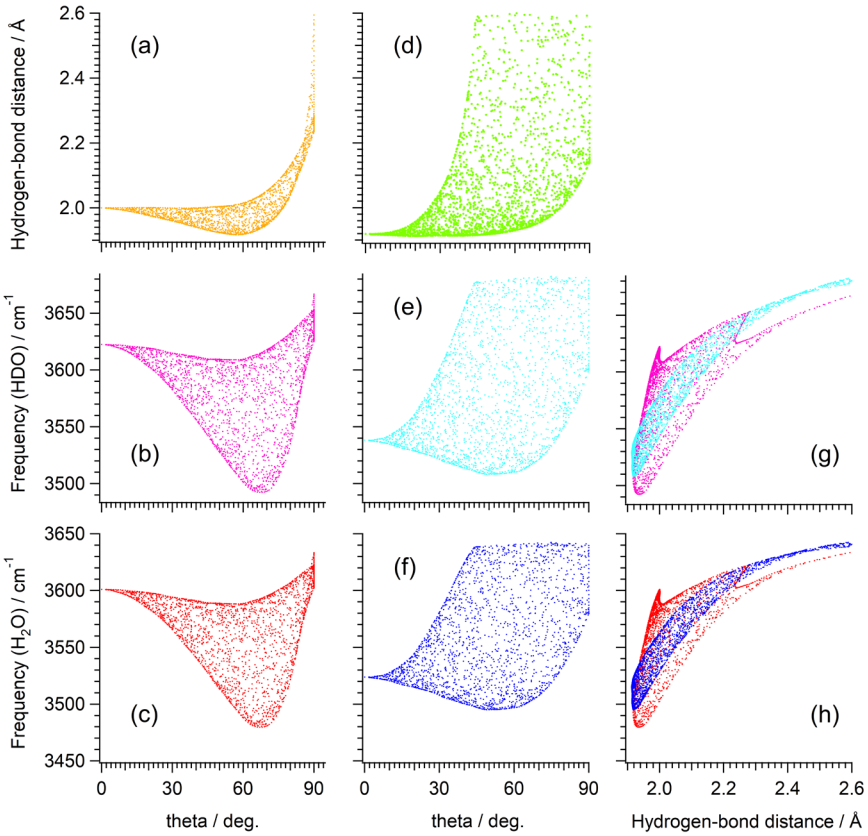

Figure S6. Plots of the (a,d) hydrogen-bond distance, (b,e,g) vibrational frequency (scaled) of the OH stretch of HDO (with the dangling bond being deuterated), and (c,f,h) vibrational frequency (scaled) of the lower-frequency OH stretch of H_2O against the (a–f) θ angle (defined in the text of this Supporting Information) and (g,h) hydrogen-bond distance calculated for the acetone + H_2O complexes with variously fixed angular hydrogen-bond configurations (orange, pink, and red dots, in panels a–c, g, and h) and for the dimethyl ether + H_2O complexes with variously fixed angular hydrogen-bond configurations (light and dark blue dots, in panels d–f, g, and h).

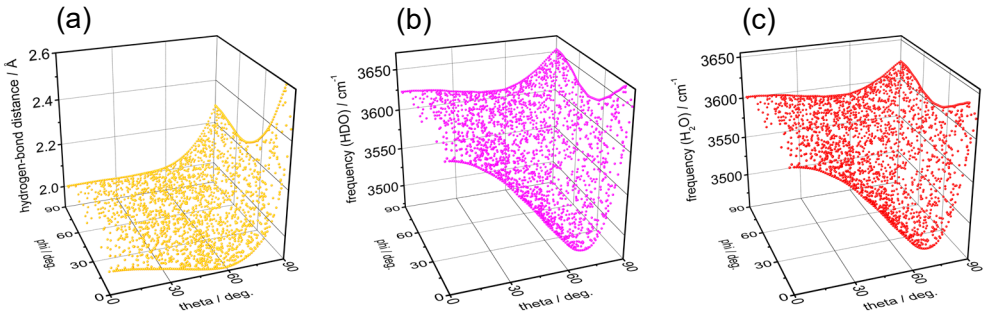

Figure S7. Three-dimensional plots of the (a) hydrogen-bond distance, (b) vibrational frequency (scaled) of the OH stretch of HDO (with the dangling bond being deuterated), and (c) vibrational frequency (scaled) of the lower-frequency OH stretch of H_2O against the θ and φ angles (defined in the text) calculated for the acetone + H_2O complexes with variously fixed angular hydrogen-bond configurations (orange, pink, and red dots).

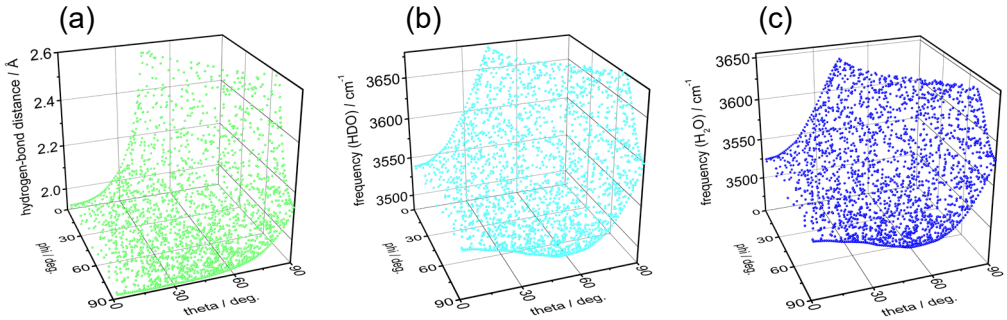

Figure S8. Three-dimensional plots of the (a) hydrogen-bond distance, (b) vibrational frequency (scaled) of the OH stretch of HDO (with the dangling bond being deuterated), and (c) vibrational frequency (scaled) of the lower-frequency OH stretch of H_2O against the θ and φ angles (defined in the text) calculated for the dimethyl ether + H_2O complexes with variously fixed angular hydrogen-bond configurations (green, light blue, and dark blue dots).

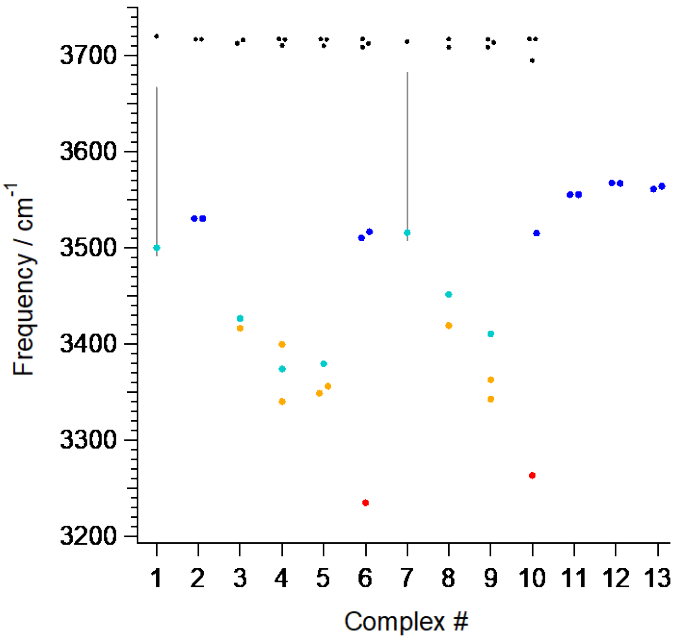

Figure S9. Vibrational frequencies (scaled) of HDO in the complexes of types 1a and 1e (numbered as 1–10 for the structures shown in part a–j of Figure S3) and type 4 (numbered as 11–13 for the structures shown in part a–c of Figure S4), calculated by deuterating all but one hydrogen atom in each complex. Each OH bond is characterized by the M value as $M = 0$ (blue), 1 (light blue), 2 (orange), and 3 (red). Stretching modes of dangling OH bonds are shown with small black markers. For some complexes, the markers are displaced horizontally to clearly show two or more closely located data. The frequency range obtained for the complexes of type 2a or 2e is also shown with a gray bar overlapped with the markers for complex 1 and 7, respectively.